Supercomputer Center. Many stimulating discussions with K. Kailasanath and F. Grinstein, both at Naval Research Laboratory, are highly appreciated.

References

[1]Lazaro, B. J., and Lasheras, J. C., "Particle Dispersion in the Developing Free Shear Layer. Pt. 1. Unforced Flow," *Journal of Fluid Mechanics*, Vol. 235, 1992, pp. 143–178.

[2]Lazaro, B. J., and Lasheras, J. C., "Particle Dispersion in the Developing Free Shear Layer. Pt. 2. Forced Flow," *Journal of Fluid Mechanics*, Vol. 235, 1992, pp. 179–221.

[3]Longmire, E. K., and Eaton, J. K., "Structure of a Particle-Laden Jet," *Journal of Fluid Mechanics*, Vol. 236, 1992, pp. 217–257.

[4]Hishida, K., Ando, A., and Maeda, M., "Experiments on Particle Dispersion in a Turbulent Mixing Layer," *International Journal of Multiphase Flow*, Vol. 18, No. 2, 1992, pp. 181–194.

[5]Chein, R., and Chung, J. N., "Effects of Vortex Pairing on Particle Dispersion in Turbulent Shear Flows," *International Journal of Multiphase Flow*, Vol. 13, No. 2, 1987, pp. 785–802.

[6]Crowe, C. T., Chung, J. N., and Trout, T. R., "Particle Mixing in Free Shear Flows," *Progress in Energy and Combustion Science*, Vol. 14, No. 3, 1988, pp. 171–194.

[7]Boris, J. P., Grinstein, F. F., Oran, E. S., and Kolbe, R. L., "New Insights into Large Eddy Simulation, Naval Research Laboratory," Naval Research Lab., NRL/MR/4400-92-6979, Washington, DC, 1992.

[8]Aggarwal, S. K., Uttuppan, J., Grinstein, F. F., and Kailasanath, K., "Particle Dispersion in a Transitional Axisymmetric Jet: A Numerical Simulation," AIAA Paper 93-0105, Jan. 1993.

[9]Hussain, Z. D., and Hussain, A. K. M. F., "Natural Instability of Free Shear Layers," *AIAA Journal*, Vol. 21, No. 11, 1983, pp. 1512–1517.

[10]Hussain, A. K. M. F., and Zaman, K. B. M. Q., "The 'Preferred Mode' of the Axisymmetric Jet," *Journal of Fluid Mechanics*, Vol. 110, 1981, pp. 39–71.

Geometry of Thin Liquid Sheet Flows

Donald L. Chubb* and Frederick D. Calfo†
NASA Lewis Research Center, Cleveland, Ohio 44135
Marc W. McConley‡
Princeton University, Princeton, New Jersey 08544
and
Matthew S. McMaster§ and Abdollah A. Afjeh¶
University of Toledo, Toledo, Ohio 43606

Introduction

INCOMPRESSIBLE, thin-sheet flows have been of research interest for many years. Those studies were mainly concerned with the stability of the flow in a surrounding gas. Squire[1] was the first to carry out a linear, inviscid stability analysis of sheet flow in air and compare the results with experiment. Dombrowski and Fraser[2] did an experimental study of the disintegration of sheet flows using several viscous liquids. They also detected the formation of holes in their sheet flows. Hagerty and Shea[3] carried out an inviscid stability analysis and calculated growth rates for the instability. They compared their calculated growth rates with experimental values. Taylor[4–6] studied extensively the stability of thin liquid sheets both theoretically and experimentally. He showed that thin sheets in a vacuum are stable. Brown[7] experimentally investigated thin liquid sheet flows as a method of application of thin films. Clark and Dombrowski[8] carried out a second-order stability analysis for inviscid sheet flows. Lin[9] introduced viscosity into the linear stability analysis of thin sheet flows in vacuum. Mansour and Chigier[10] conducted an experimental study of the breakup of a sheet flow surrounded by high-speed air. Lin et al.[11] did a linear stability analysis that included viscosity and a surrounding gas. Rangel and Sirignano[12] carried out both a linear and nonlinear inviscid stability analysis that applies for any density ratio between the sheet liquid and the surrounding gas.

Now there is renewed interest in sheet flows because of their possible application as low mass radiating surfaces.[13,14] The objective of this study is to investigate the fluid dynamics of sheet flows that are of interest for a space radiator system. Analytical expressions that govern the sheet geometry are compared with experimental results. Since a space radiator will operate in a vacuum, the analysis does not include any drag force on the sheet flow.

Theory

Sheet Thickness and Sheet Length/Sheet Width Scaling

A sketch of the flow geometry of a thin liquid sheet is shown in Fig. 1. Surface tension forces at the two edges of the sheet push the edges toward the z axis. As a result, as the flow moves in the z direction, the edge cross-sectional area A_c grows. To satisfy mass continuity, the edges approach each other and finally meet at the point $z = L$.

If sheet flow is to be utilized as a space radiator, then the dependence of the sheet length to initial width ratio L/W and sheet thickness τ on the flow conditions must be known. In this section the L/W dependence on the Weber number We will be determined. Also, since all experiments have been performed in the Earth's gravity field, the L/W and τ dependence on a constant gravity force will be included.

The surface tension force acting on the sheet edge in the x direction is given by the following[6,15]:

$$dF_x = 2\sigma\, dz \tag{1}$$

The significance of this result is that it is independent of the cross-sectional shape of the sheet. It applies as long as the edge cross section has infinite slope ($s'' \to \infty$) at the edge ($x = 0$) and zero slope ($s' = 0$) where it joins the constant thickness region ($x = r$). Combining Eq. (1) with the x direction momentum equation yields the following result for the edge velocity in the x direction[6,15]:

$$u_e = \sqrt{\frac{2\sigma}{\rho\tau}} \tag{2}$$

The velocity u_e is the velocity that a free edge of a thin liquid sheet will move regardless of the edge shape. Taylor[6] derived this result earlier without considering the cross-sectional shape of the edge. This is also the phase velocity c_{asy} of the antisymmetrical wave that can exist on a plane sheet.[5,6] It is easily shown[15] that for long sheets ($L/W > 1$) the sheet edge and stationary antisymmetrical waves (lines of constant phase) will be approximately parallel. Experimentally, these waves are observed as they have also been observed in other experiments.[3,6,10]

Equation (2) gives the sheet edge velocity u_e. With this result and the continuity equation, analytical expressions for $\tau(z)$, $x(z)$, and L/W can be developed.[15] In that derivation it is assumed that the flow velocity remains entirely in the z direction until it reaches the edge and that the gravitational force is in the z direction. With these assumptions the following result is obtained for the sheet shape:

$$\frac{2x}{W} = 1 - \frac{2}{3} Fr\sqrt{8/We}\left[\left(1 + \frac{2}{Fr}\frac{z}{W}\right)^{3/4} - 1\right] \tag{3}$$

where the Weber number We, which is the ratio of the dynamic pressure to the surface tension pressure, and the Froude number

Received July 6, 1993; revision received Dec. 22, 1993; accepted for publication Dec. 23, 1993.

*Research Engineer, Photovoltaics Branch. Member AIAA.
†Research Engineer, Aerospace Engineering Branch.
‡Student; currently Graduate Student, Massachusetts Institute of Technology, Department of Aeronautical Engineering.
§Graduate Student; currently at Virtual Engineering, St. Clair Shores, MI.
¶Associate Professor, Department of Mechanical Engineering. Member AIAA.

Fr, which is the ratio of the kinetic energy to the gravitational energy, are given by

$$We \equiv \frac{\rho w_0^2 \tau_0}{\sigma} \qquad Fr \equiv \frac{w_0^2}{gW} \tag{4}$$

When $x = 0$, the sheet flow will have reached its maximum length, $z = L$. Therefore, setting $x = 0$ in Eq. (3) yields the following result for L/W:

$$\frac{L}{W} = \frac{Fr}{2}\left[\left(1 + \frac{3}{2}\frac{1}{Fr}\sqrt{\frac{We}{8}}\right)^{4/3} - 1\right] \tag{5}$$

The importance of We in determining L/W becomes obvious when Eq. (5) is expanded for large Fr. For all of the experiments carried out to date, $Fr > 10$. For the case of no gravity field ($g = 0$), $Fr \to \infty$, and Eq. (5) yields

$$\left.\frac{L}{W}\right|_{g=0} = \sqrt{\frac{We}{8}} \tag{6}$$

Since $\sqrt{We} \sim w_0$, Eq. (6) indicates that L will be a linear function of w_0 for fixed W and τ_0. This was observed in the experiments of Mansour and Chigier[10] and Chubb and White.[13] For $Fr > 20$ there is only a small deviation from the $Fr \to \infty$ ($g = 0$) result.[15] Thus for the experimental conditions of this study, Eq. (6) can be used to estimate L/W.

Using the result of Eq. (6) for L/W in Eq. (3) yields the following equations for the sheet shape in terms of the dimensionless coordinates $2x/W$ and z/L:

$$\frac{2x}{W} = 1 - \alpha\left[\left(1 + \beta\frac{z}{L}\right)^{3/4} - 1\right] \tag{7}$$

where

$$\alpha \equiv \frac{2}{3} Fr\sqrt{8/We} \qquad \beta \equiv \left(1 + \frac{1}{\alpha}\right)^{4/3} - 1 \tag{8}$$

The quantity α can be called the sheet shape parameter since it determines the sheet shape. For most cases of experimental interest, $\alpha \geq 1$. For $\alpha \to \infty$, Eq. (7) becomes

$$\frac{2x}{W} = 1 - \frac{z}{L} \quad \text{for} \quad \alpha \to \infty \tag{9}$$

For $\alpha \geq 1$, the sheet is essentially triangular in shape.[15] Indeed, this is the result observed experimentally.

Now consider the variation of sheet thickness $\tau(z)$ (Ref.15):

$$\frac{\tau}{\tau_0} = \left(1 + \beta\frac{z}{L}\right)^{-1/2} \tag{10}$$

Similar to $x(z)$, the sheet thickness variation $\tau(z)$ depends only on the shape parameter α. Also, for no gravity force, $\beta = 0$, and Eq. (10) yields $\tau/\tau_0 = 1$; in this case the sheet thickness is a constant.

Cross-Sectional Shape of Thin Liquid Sheet

The cross-sectional shape of the sheet edge is important in evaluating the stability of the sheet. The large curvature (small radius of curvature) that exists in the region where the edge joins the sheet ($x = r$ in Fig. 1b) can lead to instability. This problem is currently being investigated.

As pointed out in the last section, the effect of the z-direction gravity force is negligible for the sheet flows of interest. Therefore, only the surface tension force must be considered. In the derivation of Eq. (3), the curvature of the sheet in the x-z plane was neglected so that the surface tension force was confined to the x-y plane. This is a reasonable assumption for flows of sufficient length ($L/W > 1$). In that case, the cross-sectional shape $s(x, z)$ increases slowly in the z direction so that $s_{xx} \gg s_{zz}$ and only curvature in the x-y plane is important.

For the most general case, however, curvature in the y-z plane must be included. In the following analysis, the velocity field is assumed to be $\boldsymbol{u} = [u(x, z), v(x, y, z), w_0]$; that is, the flow velocity is constant in the z direction, and the x component of velocity is independent of y. Assuming irrotational flow, Bernoulli's equation applied at the surface, and the continuity equation developed in Ref. 15, and using the following dimensionless variables,

$$\xi \equiv \frac{x}{\tau/2}, \qquad \eta \equiv \frac{s}{\tau/2}, \qquad \theta \equiv \frac{z}{\tau/2}, \qquad \bar{r} \equiv \frac{r}{\tau/2}, \qquad U_s \equiv \frac{u_s}{u_e} \tag{11}$$

yields the following,

$$\eta_{\xi\xi} + \eta_{\theta\theta} = \frac{1}{2}\left[\frac{1}{\eta^2}\left(\frac{\bar{A}}{\bar{A}_c}\right)^2 (1 + \eta_\xi^2) - \frac{\tau}{R_e}\right][1 + \eta_\xi^2]^{3/2} \tag{12}$$

where

$$\bar{A} = \frac{2}{\tau^2} A = \int_0^\xi \eta \, d\xi' \tag{13a}$$

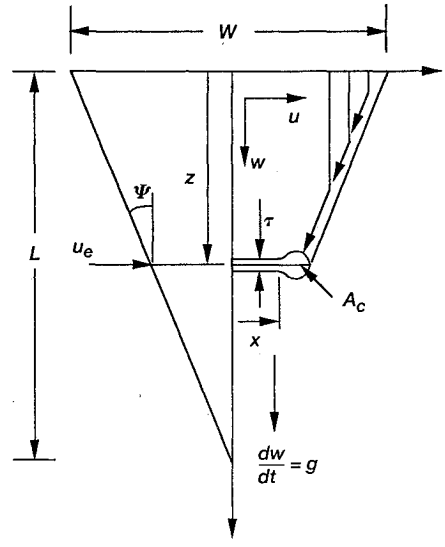

a) Top view

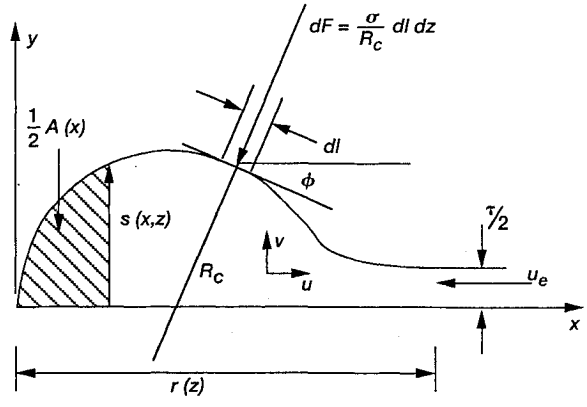

b) Sheet edge control volume in coordinate system moving with edge velocity u_e

Fig. 1 Schematic of thin liquid sheet flow.

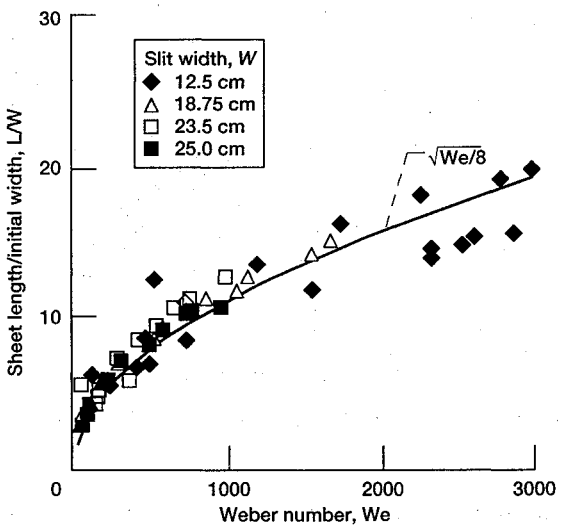

Fig. 2 Comparison of theoretical and experimental sheet scaling.

and the total dimensionless cross-sectional area of the sheet edge is

$$\bar{A}_c = \frac{2}{\tau^2} A_c = \int_0^{\bar{r}} \eta \, d\xi \tag{13b}$$

where R_e is the radius of curvature at the sheet edge ($x = 0$). In solving Eq. (12), an approximation will be made to treat $\eta_{\theta\theta}$ as an independent parameter.

As can be seen, by neglecting the η_θ terms, the only dependence on the fluid properties (ρ, σ) occurs through $\bar{A}_c$, which depends on L/W [Eq. (6)]. Thus, for a given value of A_c the sheet cross section is the same for all fluids. Solution of Eq. (12) depends on the parameters $\bar{A}_c$, τ/R_e, and $\eta_{\theta\theta}$, plus the boundary conditions $\eta = 0$ and $\partial\eta/\partial\xi \to \infty$ at $\xi = 0$ and $\eta = 1$ and $\partial\eta/\partial\xi = 0$ at $\xi = \bar{r}$. The total dimensionless cross-sectional area $\bar{A}_c$ must satisfy the condition $\bar{A}_c = \bar{A}(\bar{r})$, so that it is not a free parameter. Instead, $\bar{A}_c$ can be calculated directly from the flow conditions using the continuity equation with the $Fr \to \infty$ assumption so that $w = w_0 = w_e$ and $\tau = \tau_0$. Therefore,[15]

$$A_c = \frac{W\tau_0}{2}\frac{z}{L} \quad \text{or} \quad \bar{A}_c = \frac{W}{\tau_0}\frac{z}{L} \tag{14}$$

As already mentioned, $\eta_{\theta\theta}$ is small for the flows of interest ($L/W > 1$). However, the two sets of boundary conditions imply that two independent parameters, namely, τ/R_e and $\eta_{\theta\theta}$, are needed to obtain a physically meaningful solution. Since surface tension is presumed to act uniformly in all directions, a suitable assumption is to consider the curvature in the y-z plane to be related to the curvature in the x-y plane. This is done by setting $\eta_{\theta\theta} = \alpha\eta_{\xi\xi}$, where α is a constant that replaces $\eta_{\theta\theta}$ as a free parameter.

The iterative method for solving Eq. (12) consists of setting initial values for τ/R_e, $\eta_{\theta\theta}$, $\bar{A}_c$, and $\bar{r}$ and then using a Runge-Kutta integration routine to get revised values for $\bar{A}_c$ and $\bar{r}$. Eventually, $\bar{A}_c$ and $\bar{r}$ converge to a set of values. Since $\bar{A}_c$ is kept equal to $\bar{A}(\bar{r})$, and $\bar{r}$ is defined where $\eta_\xi = 0$, the value of η must be checked to see if it equals 1 at $\bar{r}$. If not, a new guess for $\eta_{\theta\theta}$ is made. The process is repeated until a physically meaningful solution is obtained for the value of τ/R_e assumed. Starting values for η and η_ξ in the integration are obtained by taking the limit $\xi \to 0$ in Eq. (12).[15] The Runge-Kutta algorithm reveals that solutions exist for all $\bar{A}_c$. Also, the calculated shapes are nearly elliptical.[15]

Experimental Results

In the previous studies of Chubb and White[13] and Chubb and Calfo,[14] a limited amount of scaling data was obtained. Most of those results were obtained with small slit widths ($W < 3.5$ cm).

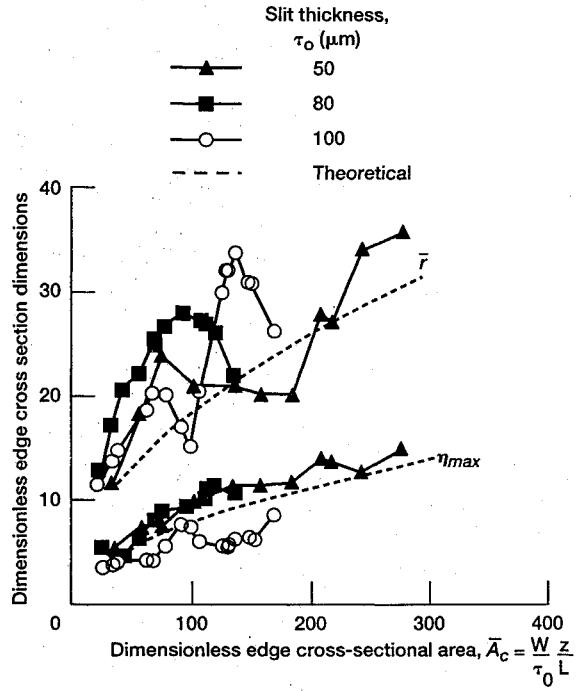

Fig. 3 Comparison of experimental and theoretical edge cross-section dimensions.

For a space radiator system, however, larger slit widths will be used. Therefore, the results reported here are for larger slit widths ($12.5 < W < 25$ cm). All of the L/W vs We data were taken using low vapor pressure Dow Corning 705 silicone oil at vacuum conditions (10^{-2} Torr). However, the edge cross-section results were done in the atmosphere using water as the working fluid. Also, the edge shape data were obtained using small slit widths.

Scaling results are shown in Fig. 2 where L/W is plotted as a function of We. These results were obtained in a large (3 m long) vacuum facility described in Ref. 15. As can be seen, the experimental data points all lie close to the calculated result, Eq. (6). The results in Fig. 2 are for vacuum conditions. However, experiments in air using water as the sheet fluid yield results that agree with Eq. (6). Only a limited range of Weber numbers ($50 < We < 300$) was investigated in the atmospheric experiments. For high-velocity flows in air, an instability will occur that breaks up the sheet flow.

The edge dimensions $\bar{r}$ and η_{max} were determined by a photographic technique.[15] These results are compared with the theoretical results in Fig. 3. A very interesting phenomenon can be seen from these results. The edge dimensions oscillate in the flow direction z. The edge begins in its nearly elliptic shape, in agreement with the theoretical prediction. Because of the high curvature where the edge connects to the sheet, the edge quickly flattens out to a "cigar-like" shape. This appears in Fig. 3 as an increase in $\bar{r}$ and a decrease in η_{max}. From photographic data[15] we know that, instead of simply regaining its elliptic shape, the edge goes through a rebuilding process where the edge has a "peanut-like" shape. As the area of the edge increases, η_{max} increases first on the inside of the previous edge. This inner part of the edge grows and engulfs the outer part to return to its elliptic shape. This appears in Fig. 3 as an increase in η_{max} and a decrease in $\bar{r}$. This is most noticeable in the 100-μm slit results.

As discussed earlier, the only edge shape solutions obtained analytically are elliptic. No peanut- or cigar-like shapes, which were observed experimentally, were calculated. Assumptions were made about the z-direction derivatives, η_θ and $\eta_{\theta\theta}$, to reduce the two-dimensional problem to a one-dimensional problem. Also, the edge shapes were assumed similar at each z location to reduce the problem to one dimension. However, the peanut- and cigar-like shapes observed indicate that the assumptions $\eta_\theta \ll \eta_\xi$, $\eta_{\theta\theta} = \alpha\eta_{\xi\xi}$, and similarity of the edge cylinders do not apply in

those cases. Solutions like the experimental cigar- and peanut-like edge shapes require a three-dimensional formulation.

References

[1]Squire, H. B., "Investigation of the Instability of a Moving Liquid Film," *British Journal of Applied Physics*, Vol. 4, June 1953, pp. 167–169.

[2]Dombrowski, N., and Fraser, R. P., "Photographic Investigation into the Disintegration of Liquid Sheets," *Philosophical Transactions*, Vol. A247, Sept. 1954, pp. 101–130.

[3]Hagerty, W. W., and Shea, J. F., "A Study of the Stability of Plane Fluid Sheets," *Journal of Applied Mechanics*, Vol. 22, Dec. 1955, pp. 509–514.

[4]Taylor, G. I., "The Dynamics of Thin Sheets of Fluid, I. Water Bells," *Proceedings of the Royal Society of London*, Vol. A253, Dec. 1959, pp. 289–295.

[5]Taylor, G. I., "The Dynamics of Thin Sheets of Fluid, II. Waves on Fluid Sheets," *Proceedings of the Royal Society of London*, Vol. A253, Dec. 1959, pp. 296–312.

[6]Taylor, G. I., "The Dynamics of Thin Sheets of Fluid, III. Disintegration of Fluid Sheets," *Proceedings of the Royal Society of London*, Vol. A253, Dec. 1959, pp. 313–321.

[7]Brown, D. R., "A Study of the Behavior of a Thin Sheet of Moving Liquid," *Journal of Fluid Mechanics*, Vol. 10, July 1961, pp. 297–305.

[8]Clark, C. J., and Dombrowski, N., "Aerodynamic Instability and Disintegration of Inviscid Liquid Sheets," *Proceedings of the Royal Society of London*, Vol. A329, May–Sept. 1972, pp. 467–478.

[9]Lin, S. P., "Stability of a Viscous Liquid Curtain," *Journal of Fluid Mechanics*, Vol. 104, March 1981, pp. 111–118.

[10]Mansour, A., and Chigier, N., "Disintegration of Liquid Sheets," *Physics of Fluids*, Vol. A2, No. 5, Nov. 1990, pp. 706–719.

[11]Lin, S. P., Lian, Z. W., and Creighton, B. J., "Absolute and Convective Instability of a Liquid Sheet," *Journal of Fluid Mechanics*, Vol. 220, Nov. 1990, pp. 673–689.

[12]Rangel, R. H., and Sirignano, W. A., "The Linear and Nonlinear Shear Instability of a Fluid Sheet," *Physics of Fluids*, Vol. A3, No. 10, 1991, pp. 2392–2400.

[13]Chubb, D. L., and White, K. A., "Liquid Sheet Radiator," AIAA Paper 87-1525, July 1987; see also NASA TM-89841, July 1987.

[14]Chubb, D. L., and Calfo, F. D., "Scaling Results for the Liquid Sheet Radiator," *Proceedings of 24th Intersociety Energy Conversion Engineering Conference* (Washington, DC), Institute of Electrical and Electronics Engineers, New York, 1989, pp. 45–50; see also NASA TM-102100, Aug. 1989.

[15]Chubb, D. L., McConley, M. W., McMaster, M. S., and Afjen, A. A., "A Study of Thin Liquid Sheet Flows," NASA TM-106323, Aug. 1993.

Effect of Damage on the Impact Response of Composite Laminates

Paul A. Lagace,* Kiernan F. Ryan,† and Michael J. Graves‡
Massachusetts Institute of Technology, Cambridge, Massachusetts 02139

Introduction

IMPACT is a key issue in the design of composite structures and may be the limiting design issue in many cases. It is therefore essential that a complete understanding of the response of composite structures to impact be obtained. This comprises two separate issues: damage resistance and damage tolerance.[1] Damage resistance is a measure of the damage incurred by a material/structure due to a particular event (in this case impact). Damage tolerance is the measure of the ability of a material/structure to "perform" (given particular performance requirements) in the presence of damage. The first issue, damage resistance, is directly related to impact. The second issue, damage tolerance, has only a secondary relationship to the impact event since it is the amount and distribution of the damage present that directly determines the damage tolerance, not the particulars of the impact event.[2] The impact event is related to damage tolerance through the damage resistance. Understanding and analyzing the damage resistance of composite structures is therefore important to determine the damage caused by a particular impact scenario. This damage state can then be used to assess the damage tolerance and thus the capability of the structure to continue to meet performance requirements.

A number of authors[1,3–9] have presented analysis techniques to determine the response of composite structures to impact. These analyses generally determine the force, deflection, and strain (and stress) time histories of the composite structure during the impact event. In some cases, the resulting damage is also predicted. Although these analysis techniques vary from the finite element method to Rayleigh-Ritz and other schemes, they all share one item in common: they do not account for the fact that the damage that occurs during the impact event is a progressive phenomenon.

The condition of a composite laminate is not constant throughout the impact event. As damage occurs during the impact event, the parameters that govern the response may change. This can influence the overall response which will alter the force, deflection, and stress and strain histories. This, in turn, can have an effect on the total amount of damage incurred during the impact event. It is therefore essential to understand how impact response parameters change as damage occurs.

The objective of this work is, therefore, to determine the effect that damage in the composite structure has on the impact response of the structure. Although quantitative measurements and assessments are made, the ultimate goal is to determine, on a qualitative basis, whether it is necessary to account for this change in impact parameters, due to damage, in models of the event and how this should be done when necessary. This overall qualitative assessment is made based on the quantitative measurements.

Approach

The impact response of laminated composites is often analyzed by segmenting the problem into the different response phenomena that occur.[1] This generally involves considering the "global" and "local" responses of the laminate promoted by the impactor. In this context, global response refers to the dynamic structural response of the laminated configuration,[10] whereas the local response refers to the indentation caused by the impactor.[11,12] Although both phenomena occur simultaneously during the impact event, the complexity of the problem is reduced by analyzing each phenomenon separately.

The effect of damage on the impact response was considered by looking at the effect of damage on both the global and local responses. The global response was assessed by conducting an impact test and measuring the force vs time and plate center deflection vs time histories. The local response was evaluated by conducting static indentation tests and measuring the load vs indentation.

All tests were conducted on AS4/3501-6 graphite/epoxy $[\pm 45/0]_{2S}$ plates 89 mm in width with a span of 251 mm. Tests were carried out on virgin (undamaged) and on predamaged specimens. Damage in the predamaged specimens was introduced by impacting laminates with a 1.53-kg impactor rod with a 12.7-mm-diam hemispherical tup at a velocity of 4.0 m/s. The amount of damage was determined from visual and dye-penetrant-enhanced x-ray techniques. This damage generally consisted of small matrix cracks on the back surface and internal damage, consisting of ma-

Presented as Paper 91-1079 at the AIAA/ASME/ASCE/AHS/ASC 32nd Structures, Structural Dynamics, and Materials Conference, Baltimore, MD, April 8–10, 1991; received Oct. 6, 1992; revision received June 8, 1993; accepted for publication June 9, 1993.

*Professor, Technology Laboratory for Advanced Composites, Department of Aeronautics and Astronautics. Associate Fellow AIAA.

†Research Assistant; currently Aeronautical Engineer, General Electric Corporate Research and Development, Schenectady, NY 12301. Member AIAA.

‡Assistant Professor; currently at The Boeing Company, Seattle, WA 98124. Member AIAA.